

# SIMULATION OF GROUND MOTION INDUCED BEAM JITTER IN THE SBLC MAIN LINAC

C. Montag\*

DESY, Notkestrasse 85, D-22607 Hamburg

*Abstract*

To keep the two beams of linear colliders in collision, the beam offset with respect to each other should be significantly below the beam size. To investigate the effect of ground motion on the beam trajectory, a ground motion simulation algorithm has been developed. This code models measurements taken at various laboratory sites and pays special attention to coherence properties of ground motion. Additionally, possible stabilization feedback algorithms are included. The code can be adapted to a broad range of vibration spectra and coherence properties. As a specific application, beam jitter in the main linac of the S-band Linear Collider SBLC has been investigated. The resulting rms beam jitter of  $\sigma_y \approx 1.3 \mu\text{m}$  corresponds to a luminosity degradation of only 1%. The jitter can be reduced to about  $0.45 \mu\text{m}$  using active stabilization of quadrupole vibrations. This indicates that, with respect to ground vibration, there is significant luminosity upgrade potential for SBLC.

## 1 GROUND MOTION SIMULATION MODELS

To simulate ground motion, two complementary algorithms have been developed[1]. Both of them can be adapted to practically any measured ground motion power spectra and coherence. The first one is based on digital filters shaping white noise random signals in order to get a realistic spectrum and correlation properties, while the second one employs fast Fourier transformations to compute ground motion signals in the time domain from the power spectra of absolute ground motion and the coherence spectra.

### 1.1 The filter-based model

The power spectrum  $P_{\text{tot}}(\omega)$  of ground motion can be roughly approximated as

$$P_{\text{tot}}(\omega) = \frac{B}{\omega^4}, \quad (1)$$

while the power spectrum of uncorrelated ground motion of two points at a distance  $L$  is described according to the *ATL* rule[2] as

$$\rho(\omega, L) = \frac{A \cdot L}{\omega^2}. \quad (2)$$

Since  $P_{\text{tot},n}(\omega) = P_{\text{corr},n}(\omega) + P_{\text{uncorr},n}(\omega) = P_{\text{tot}}(\omega)$ , with  $P_{\text{corr},n}(\omega) \geq 0$  and  $P_{\text{uncorr},n}(\omega) = \rho(\omega, L_n) \geq 0$  being the power spectra of the correlated and the uncorrelated

motion of the  $n$ th magnet with respect to the  $(n - 1)$ th at distance  $L_n$ , we get

$$\rho(\omega, L_n) \leq P_{\text{tot},n}(\omega) \quad (3)$$

for all  $n$ . Therefore, Eq. (2) has to be modified for  $\omega \geq \omega_0 = \sqrt{B/(A \cdot L)}$ [3].

Application of a first order lowpass filter with cutoff frequency  $\omega_0$  to the total motion signal of the  $n$ th magnet with power spectrum  $P_{\text{tot},n}(\omega)$  leads to[1]

$$\begin{aligned} P_{\text{corr},n+1}(\omega) &= \left| \frac{\omega_0}{s + \omega_0} \right|^2 \cdot P_{\text{tot},n}(\omega) \\ &= \left| \frac{\omega_0}{s + \omega_0} \right|^2 \cdot \frac{B}{\omega^4}, \end{aligned} \quad (4)$$

with  $s = i\omega$  being the Laplace variable. The uncorrelated part of motion of the  $(n + 1)$ th magnet with respect to the  $n$ th one results from applying a first order highpass filter to a second, independent signal with the same power spectrum  $P_{n+1}(\omega) = B/\omega^4$ [1]

$$P_{\text{uncorr},n+1}(\omega) = \left| \frac{s}{s + \omega_0} \right|^2 \cdot P_{n+1}(\omega). \quad (5)$$

In the low-frequency limit, we get

$$\lim_{\omega \rightarrow 0} P_{\text{uncorr},n+1} = \frac{A \cdot L_{n+1}}{\omega^2}, \quad (6)$$

which reflects the *ATL* rule.

As can be shown,  $P_{\text{corr},n+1} + P_{\text{uncorr},n+1} = P_{\text{tot},n+1} = B/\omega^4$ , while the resulting coherence  $|\gamma|$  can be calculated as[1]

$$\begin{aligned} |\gamma| &= \sqrt{\frac{P_{\text{corr},n+1}}{P_{\text{uncorr},n+1}} / \left(1 + \frac{P_{\text{corr},n+1}}{P_{\text{uncorr},n+1}}\right)} \\ &= \sqrt{\frac{\omega_0^2}{|s|^2 + \omega_0^2}}. \end{aligned} \quad (7)$$

To get a more realistic power spectrum, the experimental data obtained at DESY were fitted as

$$\begin{aligned} P_{\text{tot}} &= \left| \frac{B}{\omega^4} \right| \\ &+ \left| \frac{4.225 \cdot 10^{-14}}{s^2} \right| \text{ m}^2\text{Hz} \\ &+ \left| \frac{7 \cdot 10^{-6}}{s^2 + 9.425 \text{ Hz} \cdot s + 246.74 \text{ Hz}^2} \right|^2 \text{ m}^2\text{Hz}^3 \\ &+ \left| \frac{7 \cdot 10^{-7}}{s^2 + 0.528 \text{ Hz} \cdot s + 0.774 \text{ Hz}^2} \right|^2 \text{ m}^2\text{Hz}^3, \end{aligned} \quad (8)$$

\* now at KEK, Tsukuba, Japan

which in the low-frequency limit is dominated by the  $B/\omega^4$  term, leading to an  $ATL$ -like behaviour of the uncorrelated motion (Eqs. (5) and (6)).

The power spectrum and coherence measured in the HERA tunnel correspond to  $A = 4 \cdot 10^{-6} \mu\text{m}^2/(\text{m} \cdot \text{sec})$  and  $B = 3 \cdot 10^{-2} \mu\text{m}^2 \cdot \text{Hz}^3$ [4, 5]. Figure 1 shows the resulting power spectra of absolute and relative motion of two magnets at a distance of  $L=30$  m.

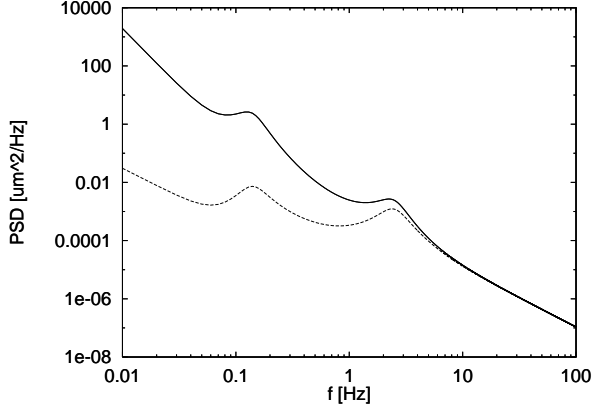


Figure 1: Power spectra (PSD) of absolute (solid line) and relative (dashed line) motion of two magnets at  $L=30$  m distance for  $A = 4 \cdot 10^{-6} \frac{\mu\text{m}^2}{\text{m} \cdot \text{sec}}$  and  $B = 3 \cdot 10^{-2} \mu\text{m}^2 \cdot \text{Hz}^3$ [1].

### 1.2 The FFT-based model

To compute the time-dependent motion signals at various points  $s_k$  along a straight line, the corresponding amplitude spectrum  $P_a(\omega)$  has to be multiplied by a phase factor function  $\exp[i(\omega t + \phi_k(\omega))]$  and inversely Fourier transformed. As can be easily shown, this leads to perfectly correlated signals  $x(t)$  and  $y(t)$  at any two points  $s_x$  and  $s_y$  for any arbitrarily chosen initial phase functions  $\phi_x$  and  $\phi_y$ ,

$$|\gamma(\omega)| = \left| \frac{\Phi(\omega) \cdot \exp[i(\phi_x(\omega) - \phi_y(\omega))]}{\Phi(\omega)} \right| = 1. \quad (9)$$

On the other hand, averaging over all neighbouring points  $s_k, s_{k-1}$  separated by the same distance  $L$  leads to[1]

$$\begin{aligned} |\gamma(\omega)| &= |\langle \exp[i(\phi_k(\omega) - \phi_{k-1}(\omega))] \rangle| \\ &= |\langle \exp[i \cdot \Delta\phi_k] \rangle|, \end{aligned} \quad (10)$$

with  $0 \leq |\gamma(\omega)| \leq 1$ . For a gaussian distribution of  $\Delta\phi_k$  with mean value  $\mu = 0$  and variance  $\sigma^2$ , and for a large number of points, this results in a coherence [1]

$$\begin{aligned} |\gamma| &= \left| \lim_{K \rightarrow \infty} \frac{1}{K} \sum_{k=1}^K \exp(i \cdot \Delta\phi_k) \right| \\ &= \exp\left(-\frac{\sigma^2}{2}\right). \end{aligned} \quad (11)$$

To compute signals with a desired correlation  $\gamma(\omega)$ , the phases  $\phi_k(\omega)$  for the motion signal at the location  $s_k$  are calculated from those at the point  $s_{k-1}$  according to

$$\phi_k(\omega) = \phi_{k-1}(\omega) + \Delta\phi_k(\omega), \quad (12)$$

with  $\Delta\phi_k(\omega)$  being normally distributed with rms value  $\sigma = \sqrt{-2 \ln(\gamma(\omega))}$  and mean value  $\mu=0$ .

Having once defined the coherence for a certain distance  $L_0$ , the coherence for any distance  $L$  results automatically according to

$$|\gamma(L)| = \exp\left(-\frac{L}{L_0} \frac{\sigma^2(L_0)}{2}\right). \quad (13)$$

The coherence measured in the HERA tunnel can be approximated by[1]

$$\begin{aligned} |\gamma(6 \text{ m})| &= \exp\left(-\frac{0.08}{2\pi} \cdot \omega\right) \\ &+ \frac{0.0028 \cdot \omega}{\sqrt{(\omega_m^2 - \omega^2)^2 + (2 \cdot \delta \cdot \omega_m \cdot \omega)^2}} \\ &+ \frac{1.05 \cdot \omega}{\sqrt{(\omega_c^2 - \omega^2)^2 + (2 \cdot \delta \cdot \omega_c \cdot \omega)^2}}, \end{aligned} \quad (14)$$

with

$$\omega_m = 2\pi \cdot 0.14 \text{ Hz}, \quad (15)$$

$$\omega_c = 2\pi \cdot 2.5 \text{ Hz}, \quad (16)$$

$$\delta = 0.2. \quad (17)$$

## 2 THE LINAC LATTICE

The S-band lattice is composed of FODO cells with constant phase advance  $\mu = 90^\circ$ . Since the accelerating sections between the quadrupoles consist of identical units of  $l=6$  m length, the scaling of the  $\beta$ -function is chosen as a stepwise function of the energy to approximate a  $\beta \propto \sqrt{E}$  scaling[6]. Figure 2 shows the scaling of the  $\beta$ -function of this lattice.

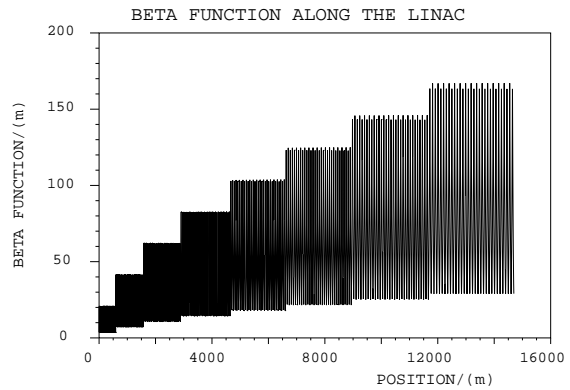


Figure 2:  $\beta$ -function scaling chosen for the SBLC main linac.

### 3 SIMULATION RESULTS

Both ground motion simulation algorithms described above have been used to determine ground motion induced beam jitter in the SBLC main linac. At the end of the main linac, a beam based correction system has been assumed which corrects the position of each bunch train by subtracting the value measured at the previous one. This can be described by the transfer function[1]

$$H(s) = 1 - \exp(-sT_0), \quad (18)$$

where  $s = i\omega$  and  $T_0$  are the Laplace variable and the time between consecutive bunch trains, respectively.

Using the FFT-based simulation algorithm, the rms beam jitter was determined to be approximately  $1.3 \mu\text{m}$ . This can be significantly reduced to about  $0.45 \mu\text{m}$  applying an active stabilization system to reduce quadrupole vibrations[7], with a transfer function shown in Fig. 3.

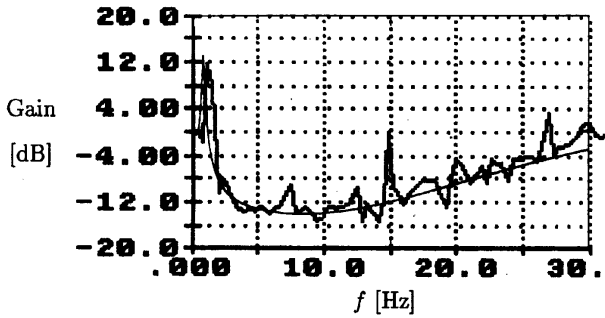


Figure 3: Measured feedback gain (thick line) of the active stabilization system in the frequency band from 0 to 30 Hz. The smooth thinner curve shows the theoretical transfer function used for the simulation[7].

From the rms beam jitter  $\sigma_y$ , the resulting luminosity  $\mathcal{L}$  in terms of the nominal luminosity  $\mathcal{L}_0$  can be expressed as

$$\mathcal{L} = \mathcal{L}_0 \cdot \exp\left(-2 \frac{\sigma_y^2}{4\sigma_{\text{beam}}^2}\right), \quad (19)$$

with  $\sigma_{\text{beam}} = 9.1 \mu\text{m}$  being the rms beam size at the end of the main linac. The obtained values correspond to luminosity degradations due to beam offset of 1% without and 0.1% with active stabilization, respectively.

Furthermore, the effect of the proportionality constant  $A$  on the luminosity was simulated using the filter-based algorithm (see Fig. 4). The rms beam jitter at  $A = 4 \cdot 10^{-6} \mu\text{m}^2/(\text{m} \cdot \text{sec})$ , the value obtained at HERA, is  $1.7 \mu\text{m}$  without and  $0.9 \mu\text{m}$  with active stabilization (Fig. 4). This is in good agreement with the results obtained using the FFT-based model.

### 4 REFERENCES

[1] C.Montag, Active Stabilization of Mechanical Quadrupole Vibrations in a Linear Collider Test Facility, Ph.D thesis, DESY 97-030.

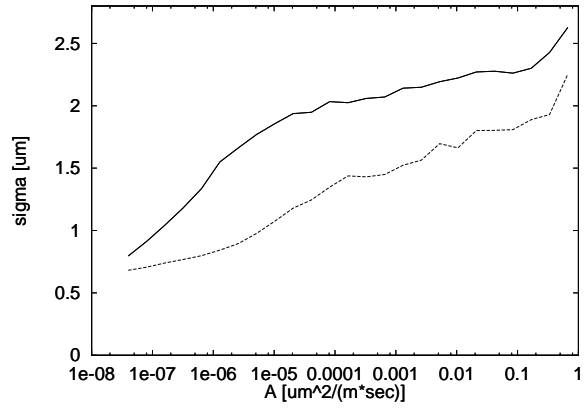


Figure 4: Resulting rms beam jitter as a function of the proportionality factor  $A$  in the  $ATL$  rule. The solid line represents the rms jitter amplitude resulting from pure ground motion, while the dashed line shows the corresponding value with active stabilization.

[2] B.A. Baklakov *et al.*, Investigation of Seismic Vibrations for Linear Collider VLEPP, Sov. Phys. ZhTF, Vol. 63, No. 10 (1993) (in Russian)

[3] A. Sery, O. Napoly, Influence of Ground Motion on the Time Evolution of Beams in Linear Colliders, Phys. Rev. E 63 (1996).

[4] V. Shiltsev *et al.*, Measurements of Ground Vibrations and Orbit Motion at HERA, DESY HERA 95-06.

[5] R. Brinkmann, J. Rossbach, Observation of Closed Orbit Drift at HERA Covering 8 Decades of Frequency, Nucl. Instr. Meth. A 350 (1994).

[6] S-Band Linear Collider SBLC Conceptual Design Report, DESY 97-048 and ECFA 97-182.

[7] C. Montag, Active Stabilization of Mechanical Quadrupole Vibrations for Linear Colliders, Nucl. Instr. Meth. A 378 (1996).